



Sharif University of Technology
Scientia Iranica
Transactions B: Mechanical Engineering
<http://scientiairanica.sharif.edu>



Research Note

Characterization of an in-house prepared magnetorheological fluid and vibrational behavior of composite sandwich beam with magnetorheological fluid core

S. Nagiredla, S. Joladarashi*, and H. Kumar

Department of Mechanical Engineering, National Institute of Technology Karnataka, Surathkal, Mangaluru, Karnataka 575025, India.

Received 16 June 2021; received in revised form 9 September 2021; accepted 14 November 2022

KEYWORDS

Magnetorheological fluid;
Rheological properties;
Driving frequency;
MR sandwich beam;
Carbon/epoxy composite.

Abstract. In the present work, two different compositions of Magnetorheological (MR) fluid samples with 24 and 30% volume fractions of Carbonyl Iron (CI) particles are prepared. The MR fluid samples contain CI particles as a dispersive medium, silicone oil as a carrier fluid, and white lithium grease as an anti-settling agent. The effects of oscillating driving frequency, strain amplitude, magnetic field, and the percentage of CI particle on the rheological properties of the MR fluid samples are presented. The properties of MR fluid samples are utilized to design and model the carbon/epoxy composite sandwich beams using the ANSYS Composite Pre-post (ACP) module. The modal, harmonic, and transient analyses are performed on all the modeled sandwich beams to study the influence of MR fluid core thickness, face layer thickness, CI particles volume percentage, and magnetic field on the vibrational response of the sandwich beams. The present study shows significant results in the vibrational response of the composite sandwich beam, which will be more useful for structural applications.

© 2023 Sharif University of Technology. All rights reserved.

1. Introduction

Magnetorheological (MR) fluids fall into the smart materials category, which shows a significant change in its rheology when an external magnetic field is supplied. MR fluid was reported for the first time by Rabinow

in 1948 [1]. MR fluid typically contains CI particles (20–40 vol%), carrier fluid (60–80 vol%), and an anti-settling agent (additive). CI particle size used in MR fluid typically varies in the range of 1–10 μm [2–4]. The MR fluid can change its yield stress and viscosity very quickly through the application of an external field. The MR fluid response is in the range of a few milliseconds in the presence of external stimuli, and it is capable of producing higher yield stresses based on the CI particle volume percentage and an external field applied [5,6]. Because of the fast, controllable rheological properties and reversible quality of the MR fluid, they found many potential applications in the

*. Corresponding author. Tel.: 0824 247 3722
E-mail addresses: suryarao914@gmail.com (S. Nagiredla);
sharnappaj@nitk.edu.in (S. Joladarashi);
hemanta76@gmail.com (H. Kumar)

field of vibration control devices, dampers, brakes, and clutch applications. MR fluid potential applications and basic characteristic properties were presented [4,7–9]. The rheological properties like storage modulus, loss modulus, and loss factor of Electro-Rheological (ER) fluid were discussed and the influence of magnetic field on rheological properties was presented [10–12]. The rheological properties of the MR fluid under the impact of different parameters were discussed [13,14]. The performance comparison for MR and ER fluids in adaptive beams was discussed at different magnetic and electric field values [15,16]. The use of MR/ER fluids in sandwich beam applications was discussed and also, the current status of experimental and numerical techniques for the sandwich beam response was presented [17,18]. The theoretical/experimental studies were conducted on the MR elastomer sandwich beam to study the influence of the magnetic field on the dynamic response [19,20]. The vibration suppression capability of MR fluids in the sandwich beams was investigated by fabricating the sandwich beams. There is a significant reduction in vibration amplitude reported [21,22]. The dynamic response of the MR composite laminated beams using the Finite Element (FE) method was discussed, and the influence of MR fluid core thickness on the vibrational response was studied [23–25]. Vibration suppression capabilities of MR fluid in sandwich beams were presented with the experimental, FE formulations, and Ritz method. The results exhibited significant vibration suppression capabilities for the MR sandwich beams [26,27]. The experimental studies on the dynamic behavior of the MR fluid sandwich beams with different composite face layers were conducted and the reasonable vibration amplitude reduction with the applied magnetic field was observed [28,29]. To sum up the literature, there are very few studies documented on the rheological properties of the MR fluid in the pre-yield region. Despite this, very few studies have been reported on the use of in-house prepared MR fluid samples for the sandwich beam structures. In the present work, two different MR fluid samples are prepared to study the rheological properties in the pre-yield region. The impacts of magnetic field and the volume percentage of iron particles on the rheological properties of in-house prepared MR fluids are reported. The dynamic behavior of the MR sandwich beam is explored in both frequency and time domains by utilizing the properties obtained from the rheological study of the MR fluid samples. Further, the impacts of the MR fluid core thickness, face layer thickness, CI particles volume percentage (%), and magnetic field on both the natural frequency and transient behavior are studied to address the vibration suppression capabilities for the MR fluids in the sandwich beam applications.

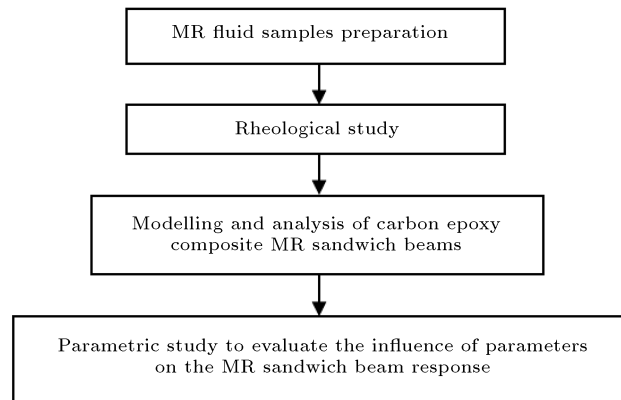


Figure 1. Methodology followed for this research work.

2. Methodology

The methodology followed for this particular research work is shown in Figure 1. The methodology involves preparation of in-house MR fluid samples, rheological study, modeling and analysis of carbon epoxy composite MR sandwich beams, and a parametric study to evaluate parameters that influence the response of the MR sandwich beam.

2.1. Materials and equipment used for the preparation of MR fluid samples

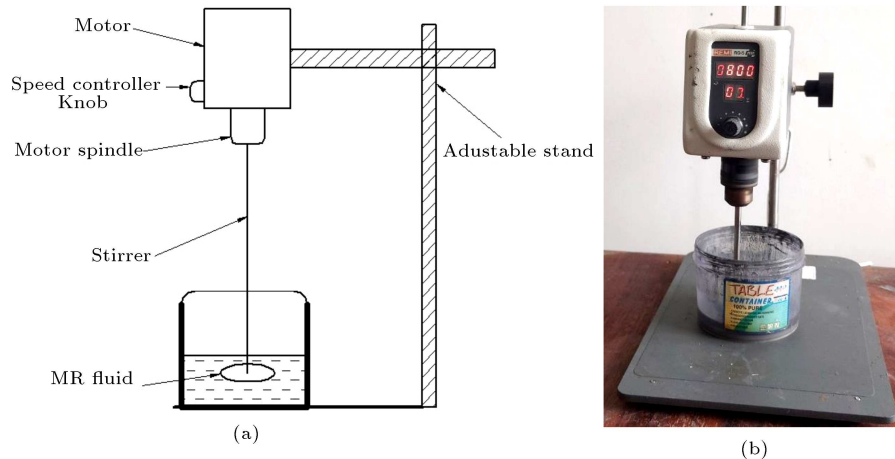
The MR fluid contains iron powder particles suspended in the carrier fluid medium. In this work, the used iron particles are CI particles and silicone oil is considered as the carrier fluid. The CI particles, low in magnesium and manganese compounds with a purity of 99.5%, were purchased from Sigma Aldrich with a density of 7.86 g/cm^3 . The viscosity of the silicone oil is 340 Cst (at 25°C), and the density is 0.970 g/cm^3 (at 25°C), which was supplied by Merck Life Science Private Limited. Additionally, a small amount of white lithium grease is used as a surfactant (surface modifier or additive) to avoid the sedimentation of the iron particles. White lithium grease, which is a paste-like substance, was bought from Permatex. This surfactant accumulates around the iron particles to keep them afloat in the carrier fluid. Two types of MR fluid samples are prepared with different compositions of CI particles, as given in Table 1.

2.2. MR fluid preparation procedure

The MR fluid samples are prepared at room temperature. The S-I and S-II MR fluid samples are prepared with the compositions, as shown in Table 1. Volume fraction calculations are used to prepare MR fluid samples. The desired volume fractions are converted into weight fractions using the density property of iron particles and silicone oil. The weight fractions of the materials are easy to measure using the weighing machine. The weight fraction proportions for both the samples are measured using high precision weighing

Table 1. MR fluid samples composition.

SI. no.	Volume percentage (vol%)		Additive (vol%)
	CI particles	Silicone oil	White lithium grease
S-I	30	70	0.5
S-II	24	76	0.5

**Figure 2.** (a) Line diagram of the mechanical stirrer and (b) MR fluid preparation using a mechanical stirrer.

machine tool. For S-I MR fluid sample, 44.8 grams of silicone oil is taken in the container. Then, the container that contains the carrier fluid is kept under a Mechanical stirrer. REMI RQ-5 Plus mechanical type stirrer is used for the stirring of MR fluid. The stirrer shaft or rotator of the mechanical stirrer is arranged in such a way that it should not touch the base of the container. Initially, 0.5% of white lithium grease is added to the carrier fluid while stirring. The speed maintained for this stirring process is 600 rpm. This process is continued for 2 hours for the uniform mixing of an additive in the carrier fluid. Then, 155.2 g of CI particles are added in small amounts while the fluid is stirred at 800 rpm. This stirring process is continued for at least 12 hours without interruption for uniform mixing of CI particles in the carrier fluid. For the S-II MR fluid sample, 56.24 g of silicone oil, 0.5% of white lithium grease, and 143.76 g of CI particles are taken. A similar procedure is followed for the preparation of the S-II MR fluid sample. The mixing process of silicone oil and white lithium grease without adding CI particles turns the silicone oil into white color. The whitish color indicates the uniform mixing of white lithium grease in the carrier fluid. After this mixing process, the fluid is turned into black color because of the added CI particles. The diagram of the mechanical stirrer and MR fluid sample preparation process using the mechanical stirrer are shown in Figure 2(a) and (b), respectively.

2.3. The microstructure of CI particles

Scanning Electron Microscopy (SEM) and Particle Size

Distribution (PSD) tests are performed on CI particles to confirm the surface morphology and particle size [28,22]. Figure 3(a) shows the density distribution (%) and cumulative value (%) histogram with the particle size diameter. Figure 3(b) shows the iron particle shape that is viewed at 25000 \times using SEM analysis. From the SEM analysis, it is observed that iron particles are spherical. The SEM and PSD suggest that the average iron particle size is around 5 to 9 μm as the supplier provided in the product catalogue.

3. Rheological experimental setup

The rheological characterization of the prepared MR fluid samples is performed using a Modular Compact Rheometer (MCR 702 Anton Paar make), as shown in Figure 4. The measuring system includes mainly Magnetorheological Device (MRD) cell for proving an external magnetic field, data processing sensors connected to the rheometer, and RheoCompassTM software to acquire the data from the sensors of the rheometer. For rheometry testing, a flat plate-type configuration is used. A measuring gap of 0.5 mm is used for all the rheometer tests. For every test, approximately 0.4 ml of the fluid sample is filled in the gap of the configuration of two parallel plates.

4. MR sandwich beam design and modelling

The ANSYS Composite Pre-post (ACP) module is used for the design and modeling of the composite sandwich beams. The composite sandwich beams are modeled

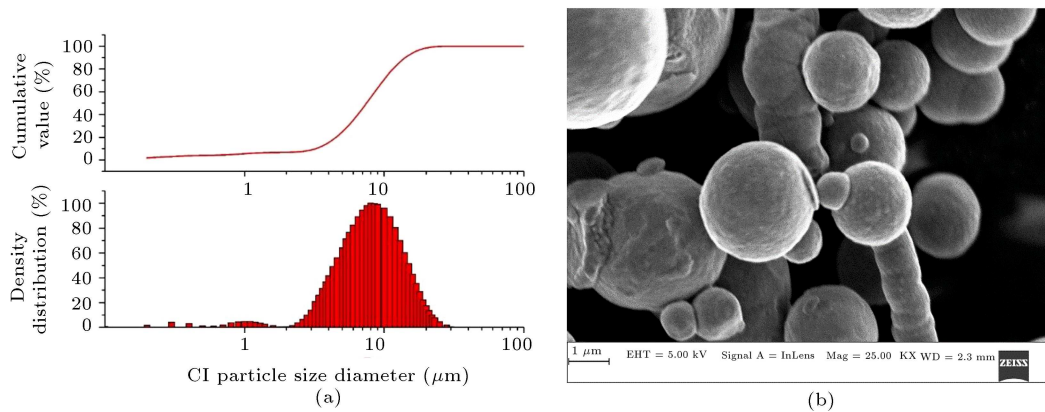


Figure 3. (a) PSD and (b) SEM analysis of the CI particles.



Figure 4. Rheometer (Anton Paar MCR 702) experimental setup with MR cell.

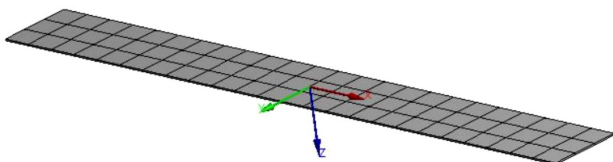


Figure 5. The generated mesh of the designed composite beam.

with the carbon/epoxy composite face layers and the MR fluid core. The shell structure is required to be created before proceeding to sandwich beam design, as shown in Figure 5. The ASTM E756–05 standard [30] is followed to design and model all the MR fluid sandwich beams with dimensions of 220 mm in length and 25 mm in width. The mesh is generated with the quad4 elements, and the aspect ratio is used to check the element quality of the generated mesh, as shown in Figure 6. Aspect ratio is the parameter for measuring the deviation of meshed elements from having the equal length of sides. The aspect ratio of the meshed elements close to ‘one’ is preferred for the best and most accurate simulation results. The aspect ratio of the meshed beam for the present work is near

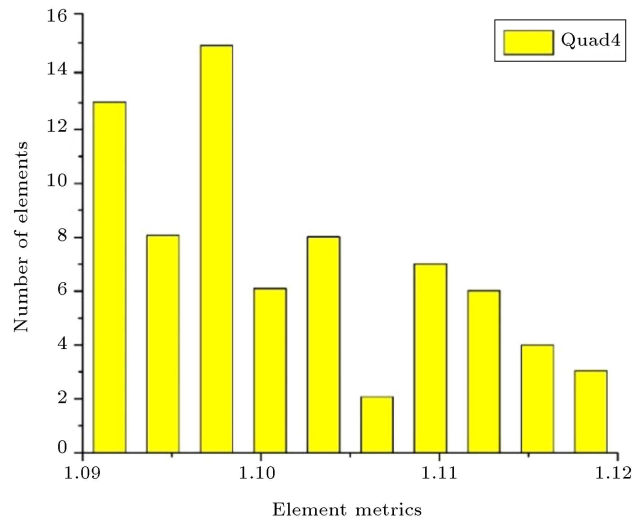


Figure 6. The aspect ratio for the meshed elements of the composite beam.

one, which means that the generated mesh quality is good. The designed composite sandwich beam contains two layers of the composite face layers at the bottom and top and MR fluid core layer in the middle, as

Table 2. Dimensions of different composite sandwich beam specimens.

Specimen	Top and bottom face layer thickness ($h_1 = h_3$) (mm)	MR fluid core thickness (h_2) (mm)	Total thickness of the composite sandwich beam (mm)
Type-I	0.6	1	2.2
	1.2		3.4
	1.8		4.6
	2.4		5.8
	3.0		7
Type-II	0.6	2	3.2
	1.2		4.4
	1.8		5.6
	2.4		6.8
	3.0		8
Type-III	0.6	4	5.2
	1.2		6.4
	1.8		7.6
	2.4		8.8
	3.0		10

Table 3. Properties of carbon/epoxy composite material and MR fluid.

Material	Density (kg/m^3)	Shear modulus (Pa)	Poisson's ratio	Elastic modulus (GPa)
Carbon/epoxy composite material	1514	$G_{12} = \frac{E_1}{2(1+\nu_{12})} = 24.008 \times 10^9$	$\nu_{12} = 0.25$	$E_1 = E_2 = 60.02$
MR fluid	3500	S-II MR fluid sample: $1.0986 \times 10^6 + 2.40817 \times 10^6(B)$	$\nu = 0.3$	-
		S-I MR fluid sample: $1.60168 \times 10^6 + 3.3731 \times 10^6(B)$		

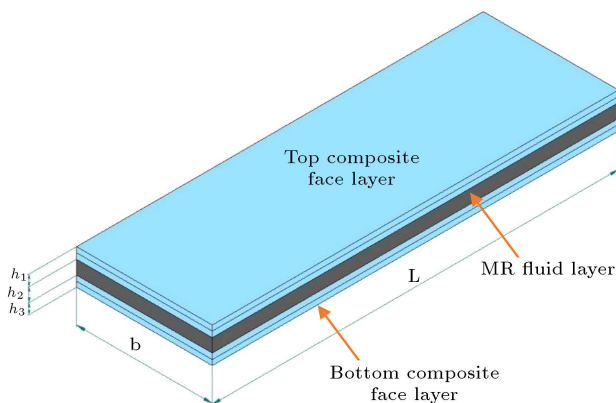


Figure 7. Designed composite sandwich beam.

shown in Figure 7. The thickness of each composite face layer is 0.6 mm. The details of the designed composite sandwich beams with different thicknesses are tabulated in Table 2. The properties used to model

the MR sandwich beam with carbon/epoxy composite face layer are tabulated in Table 3.

5. Results and discussion

The current sweep (0 to 5A) at a constant shear rate of 1/s is performed to find the relation between the applied current and the developed magnetic field. For every MR fluid, there exists a relationship between the applied current and the magnetic field produced. For MRF-132LD, the linear relation exists [13]. This direct relationship may not be well fitted for the other fluids. Based on the results obtained, Figure 8(a) shows the linear relation between applied current and the magnetic flux developed for the prepared MR fluid. Further, the variation in viscosity with the current is illustrated in Figure 8(b). The viscosity of MR fluid is increased rapidly up to 2A of current. After that, the change in the viscosity curve is minimal

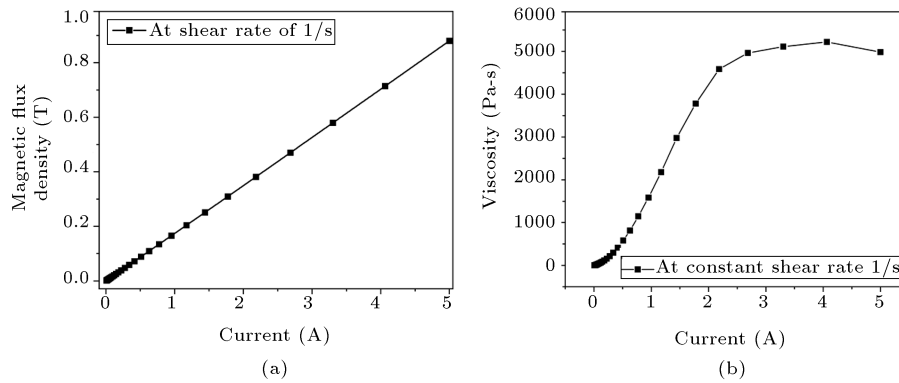


Figure 8. (a) Magnetic flux density and (b) viscosity with the current.

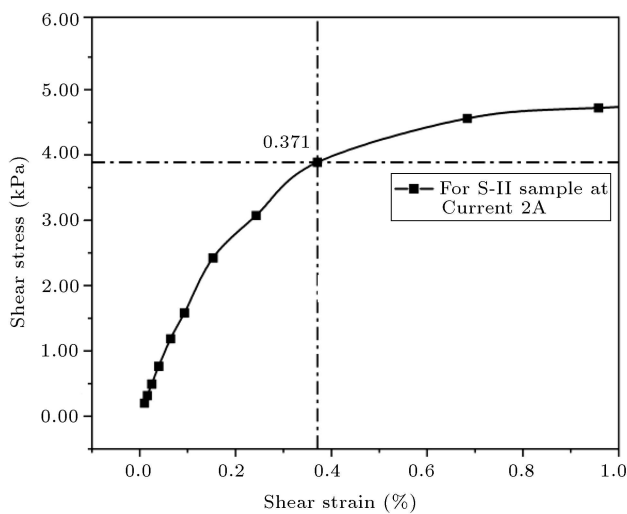


Figure 9. Shear stress-strain curve to find the yield strain.

and almost constant. This indicates that there will not be much improvement in the fluid viscosity, even if the current is increased further. The MR fluid exhibits linear viscoelasticity when the developed shear strain for the fluid is within the region of yield strain amplitude. The oscillatory shear strain amplitude test is performed at 2A of current to determine the yield strain. The amplitude sweep is applied logarithmically up to 1% shear strain amplitude. The yield strain of 0.371% is determined for the prepared MR fluid sample, as shown in Figure 9. The obtained yield strain for the prepared MR sample is in good agreement with the yield strain obtained in the research work [12,13]. For further experiment, the maximum shear strain amplitude ($\gamma_0 = 0.04\%$) is applied to ensure the obtained results are within the pre-yield region.

5.1. Frequency-dependent rheological properties

The frequency sweep is conducted at a constant shear strain amplitude ($\gamma_0 = 0.04\%$). The frequency sweep is applied logarithmically from 1 to 100 Hz. Figure 10(a) and (b) illustrate the variation of storage modulus and

loss factor with driving frequency in different magnetic fields. The storage modulus increases, while the loss factor value decreases as the applied magnetic field increases. In lower magnetic fields, all the CI particles in the MR fluid sample may not be in alignment properly and there is a more fluidity in the MR fluid sample. This issue causes significant loss factor in low magnetic fields. In higher magnetic fields, the iron particles in the fluid are arranged appropriately in a particular direction and the fluid becomes semi-solid. This arrangement will restrict the iron particle movement in the MR sample. This might decrease the loss factor value at a particular driving frequency with the applied field.

5.2. Amplitude strain-dependent rheological properties

An amplitude strain sweep test is conducted at a constant angular frequency of 10 rad/sec. The amplitude sweep is applied logarithmically from 1 to 10% strain amplitude. Figure 11(a) and (b) show the variation in storage modulus and loss factor with strain amplitude, respectively. The storage modulus of the MR sample is reduced, and the loss factor is increased as the strain amplitude increases from 1 to 10% of shear strain. The amplitude strain-dependent properties including storage modulus and loss factor obtained in this research work are in good agreement with those in the referenced research work [13].

5.3. Magnetic field-dependent rheological properties

The magnetic field-dependent storage modulus and loss factor at different driving frequencies 10 Hz, 20 Hz, 40 Hz, 70 Hz, and 100 Hz at a constant 0.04% of the amplitude of strain are plotted as shown in Figure 12(a) and (b), respectively. All the results presented in this section are taken from the frequency sweep test. The storage modulus at any driving frequency is increased with the applied magnetic field value. The iron particles in the MR fluid begin to be arranged in a chain-like structure with the applied magnetic field value.

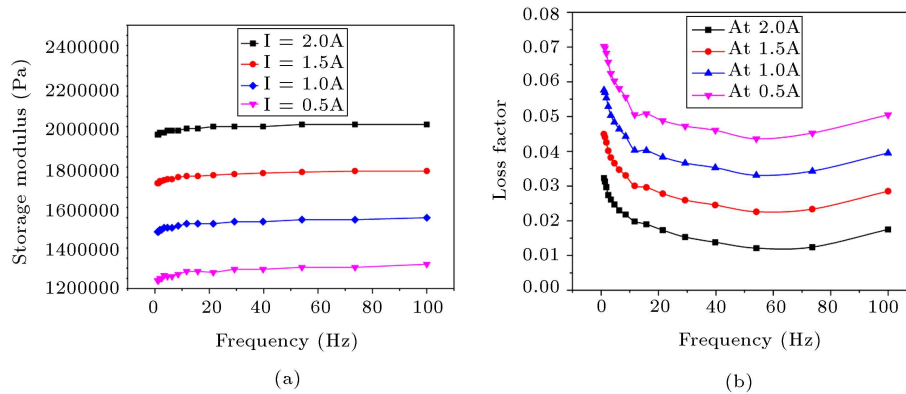


Figure 10. Frequency dependency of (a) storage modulus and (b) loss factor at different currents.

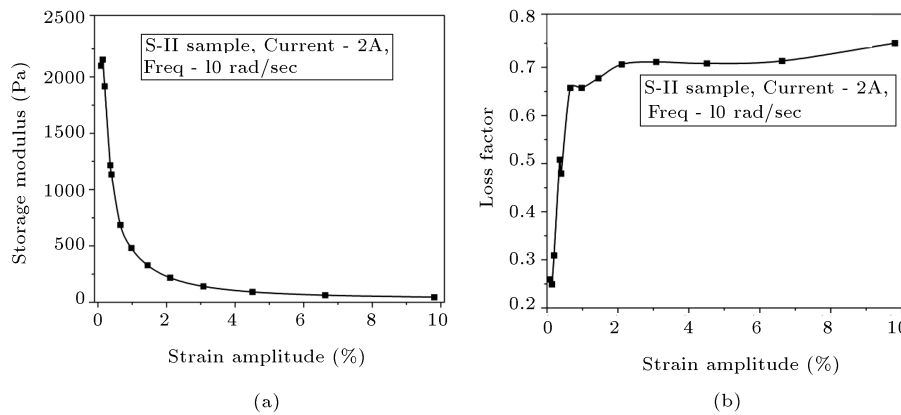


Figure 11. Strain amplitude dependency: (a) Storage modulus and (b) loss factor at 2A current.

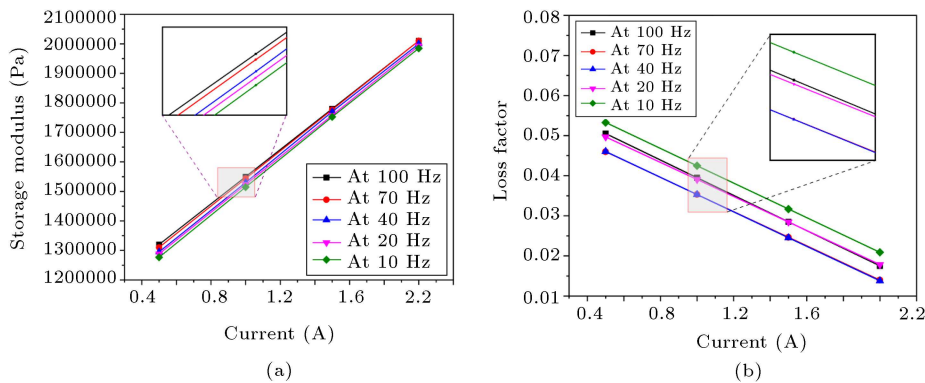


Figure 12. Magnetic field dependency: (a) Storage modulus and (b) loss factor at different driving frequencies.

The MR fluid changes its rheological properties due to changes in the arrangement of iron particles in the MR fluid. At 100 Hz of frequency, the storage modulus value is higher than the 10 Hz driving frequency at the same applied field value. The storage modulus value is increased with the driving frequency in any particular magnetic field. However, the loss factor value is reduced with the applied field value at any driving frequency, as shown in Figure 12(b). The loss factor value at any particular magnetic field is initially decreasing, followed by increase as the driving frequency increases.

5.4. Volume fraction dependent rheological properties

The dependency of MR fluid rheological properties on the volume percentage of CI particles is presented in this section. The storage modulus and loss factor for the S-I and S-II samples are shown in Figure 13(a) and (b), respectively. The storage modulus of S-II sample is greater than that of the S-I MR fluid sample. For the applied magnetic field value, the MR effect is greater at the higher vol% of CI particle MR fluid sample. However, the loss factor value for the S-I is lower than that for the S-II MR fluid sample. From the

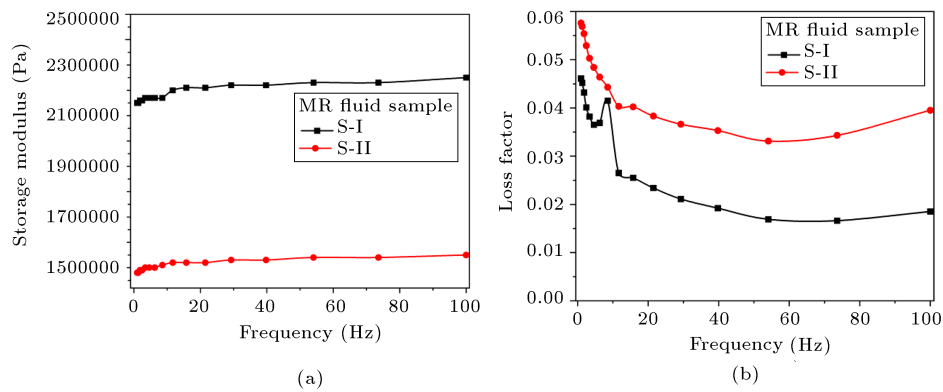


Figure 13. Volume fraction dependency: (a) Storage modulus and (b) loss factor for S-I and S-II samples with frequency.

results obtained in this work, it is confirmed that iron particle concentration in the MR fluid strongly affects the rheological properties.

5.5. Estimation of storage modulus and loss factor equations

The storage modulus and loss factor are formulated in terms of magnetic field based on the experimental results. The linear regression is used for the estimation of equations in terms of magnetic field.

The complex shear modulus of the MR fluid is given as:

$$G^*(B) = G'(B) + iG''(B), \tag{1}$$

where the real part $G'(B)$ is the storage modulus and the imaginary part $G''(B)$ is the loss modulus of the MR fluid. Here, B is in Tesla. The loss factor is written as follows:

$$\eta(B) = \frac{G''(B)}{G'(B)}. \tag{2}$$

The equations are formulated in the pre-yield linear region of the in-house prepared MR fluid. The estimated storage modulus and loss factor equations for the prepared fluid are shown in Table 4.

The cantilever boundary condition is used for all the designed MR fluid sandwich beams. The modal, harmonic, and transient analyses are performed using ANSYS to get the vibration response of the sandwich beam. Modal analysis for the sandwich beams is performed to find the fundamental frequencies. For all the sandwich beams, the first three fundamental modes have been taken. The harmonic analysis is performed to study the vibrational response of the sandwich beam

with respect to the frequency. For harmonic analysis, 2 N force is applied at the free end of the sandwich beam, and frequency sweep is given from 0 to 1000 Hz. The transient analysis is performed to find the vibrational response in the time domain [31,32]. For the transient analysis, the step time is 0.01 seconds and the step end time is 5 seconds.

5.6. Impact of MR fluid core thickness

The MR fluid core thickness affecting the vibration response is presented at a constant magnetic field density of 600 G and by maintaining the thickness of constant face layers of 1.2 mm. The change in the thickness of the MR fluid core influenced both the natural frequency and settling time response of the sandwich beam. As the core material thickness increases, both the natural frequency and vibration amplitude response of the sandwich beam decrease [26]. The amplitude-frequency plot of the MR fluid sandwich beam with 1, 2, and 4 mm core thicknesses is shown in Figure 14(a). The settling time is enhanced upon increase in the thickness of the MR Fluid core, as shown in Figure 14(b). The variation of natural frequency for the first three fundamental modes is illustrated in Figure 14(c). The variation in the natural frequency for the first mode is less than the variation in the third mode, and the difference in natural frequency is increased with the mode number.

5.7. Influence of composite face layer thickness

The carbon/epoxy composite material is used as the face layer for the MR fluid sandwich beam. The thickness of each carbon/epoxy composite layer is

Table 4. Storage modulus and loss factor equations of MR fluid samples.

Property	S-II MR fluid sample	S-I MR fluid sample
Storage modulus	$1.0986 \times 10^6 + 2.40817 \times 10^6(B)$	$1.60168 \times 10^6 + 3.3731 \times 10^6(B)$
Loss factor	$0.06149 - 0.11019(B)$	$0.05766 - 0.13321(B)$

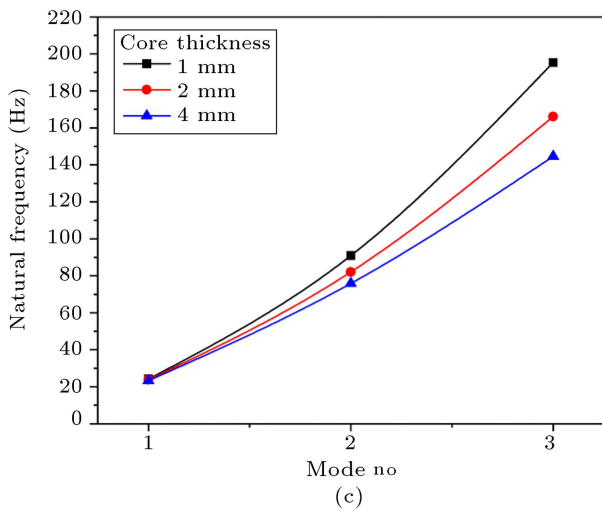
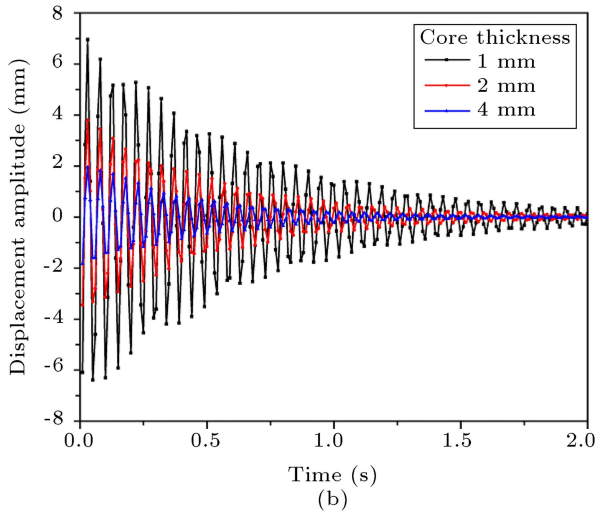
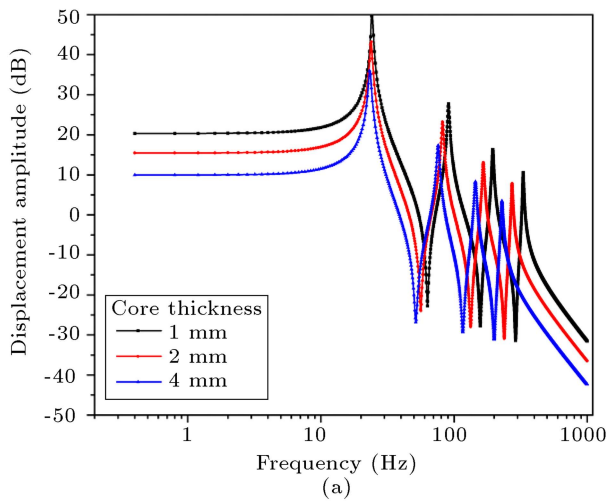


Figure 14. Influence of MR fluid core thickness on vibration response (a) amplitude versus frequency, (b) amplitude versus time, and (c) natural frequency versus mode.

0.6 mm. There is a considerable increment in the natural frequency of the sandwich beam as the composite face layer thickness is increasing, as shown in Figure 15(a). The stiffness of the sandwich beam increases

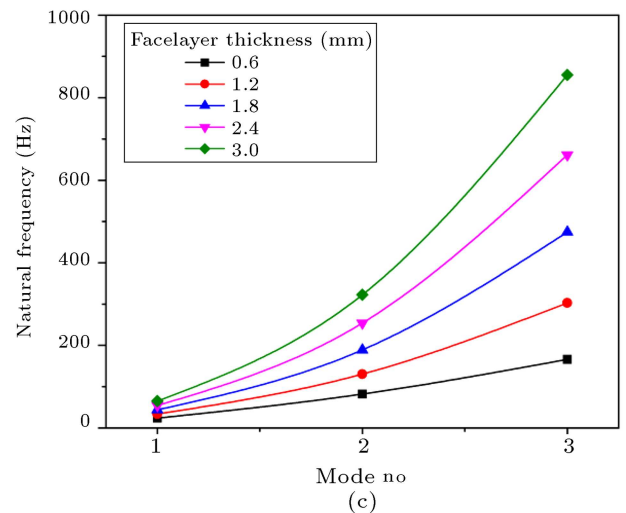
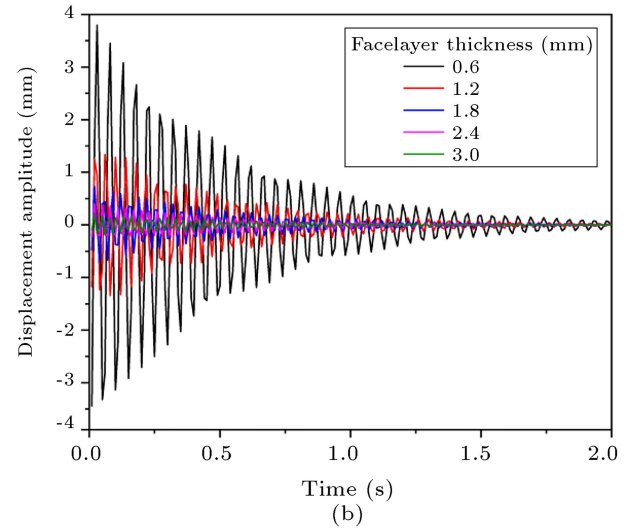
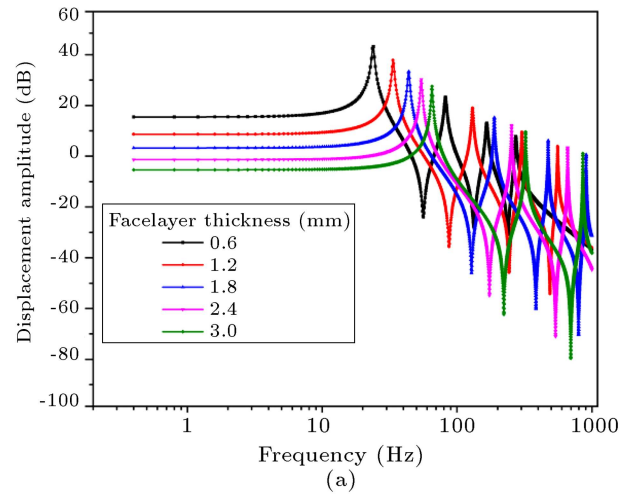


Figure 15. Influence of face layer thickness on vibration response in terms of (a) amplitude vs. frequency, (b) amplitude versus time, and (c) natural frequency vs. mode.

with the addition of more face layers, leading to the increment in the natural frequency of the MR fluid sandwich beam, as shown in Figure 15(c).

5.8. Influence of CI particles volume percentage

The impact of CI particle volume percentage on the vibration response is considered at a constant magnetic field density of 600 G by maintaining the thickness of constant face layers of 0.6 mm and MR fluid core thickness of 2 mm. As the percentage of CI particles in the MR fluid sample increases, there is a significant right shift in the frequency curve of the MR fluid sandwich beam. It is indicated that as the volume percentage of CI particles increases, there is an increment in the stiffness of the sandwich beam, as shown in Figure 16(a) and (c). An increase in stiffness influences the natural frequency of the MR fluid sandwich beam. There is a significant improvement in the settling time of the sandwich beam with the increment in the CI particle volume percentage in the MR fluid.

5.9. Influence of magnetic field

The effect of the magnetic field in the different magnetic fields on the vibration response of the MR fluid sandwich is performed by maintaining the constant face layers thickness of 0.6 mm and core thickness of 2 mm. The magnetic flux densities 0 G, 600 G, 1000 G, 1500 G, and 2000 G values are used to study the influence on the sandwich beam response. The natural frequency values of the MR fluid sandwich beam for the MR fluid samples in different magnetic fields are tabulated in Table 5. The natural frequency of the MR sandwich beam is increased with the magnetic field for all the modes. At higher modes, the change in the natural frequency is higher than in the natural frequency at lower modes. Figure 17 shows the natural frequency with respect to the magnetic field for two MR fluid samples. There is an increment in the natural frequency with CI particle volume percentage in the MR fluid in all the magnetic fields. Figure 18 shows the first three fundamental mode shapes of the cantilever MR sandwich beam. These modes correspond to the fundamental frequencies. Further, the percentage increase in the natural frequency of the MR fluid sandwich beam with respect to the applied magnetic field is calculated for the first three fundamental modes, as shown in Figure 19. The percentage of change in natural frequency is increasing as the magnetic field increases to higher values. The applied magnetic field changes the rheological properties of the MR fluid. The shear modulus of the MR fluid increases with the applied magnetic field, resulting in change stiffness of the MR fluid layer. The thickness ratio (h_2/h_1) influences the natural frequency and settling time of the MR fluid sandwich beam are shown in Figure 20(a) and (b), respectively. For all the modes, the natural frequency of the MR fluid sandwich beam is reduced as the thickness ratio increases. At the same time, settling time also decreases as the thickness ratio increases.

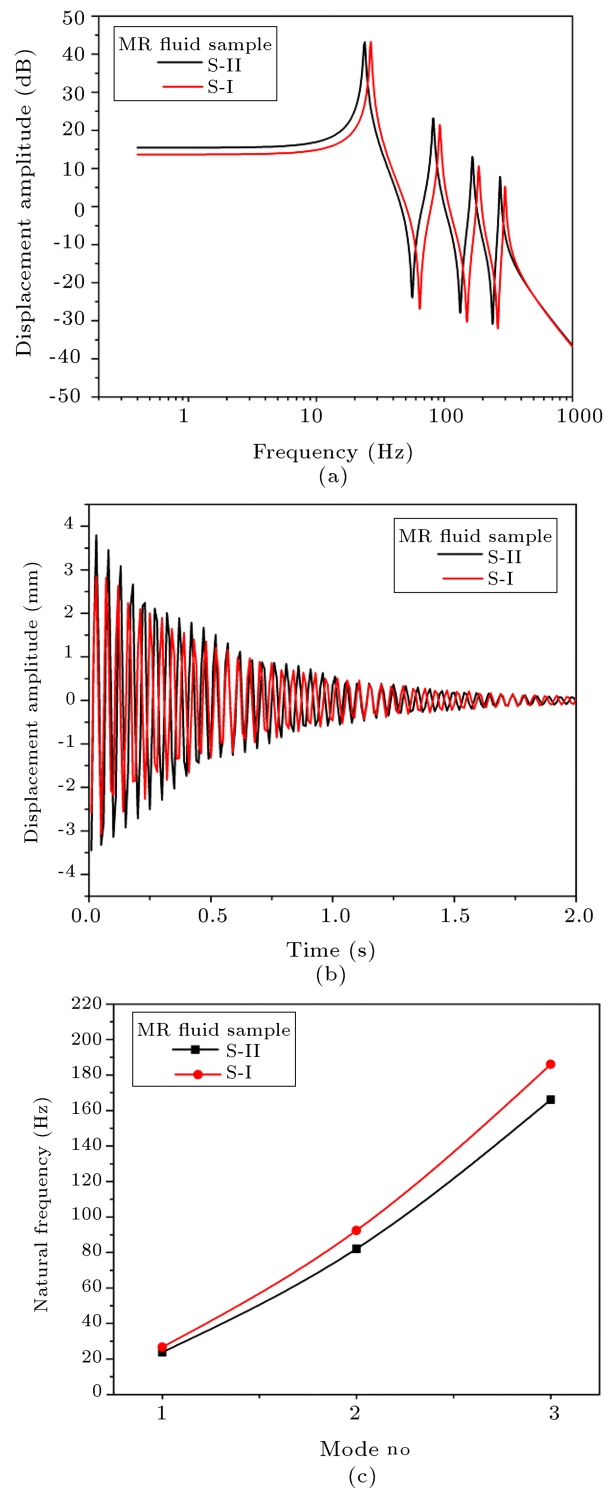


Figure 16. Influence of CI vol% in the MR fluid on the vibrational response in terms of (a) amplitude vs. frequency, (b) amplitude vs. time, and (c) natural frequency vs. mode.

6. Conclusions

The present work determined the rheological properties of the prepared Magnetorheological (MR) fluid samples in pre-yield region. The modal, harmonic, and

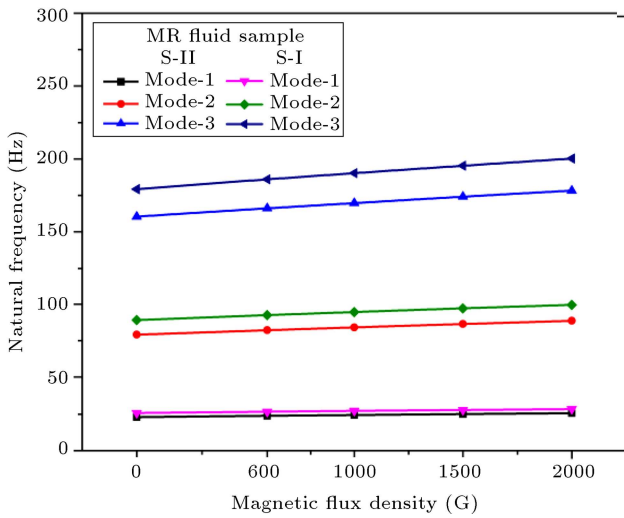


Figure 17. Natural frequency variation for the prepared MR fluid samples with the applied magnetic field.

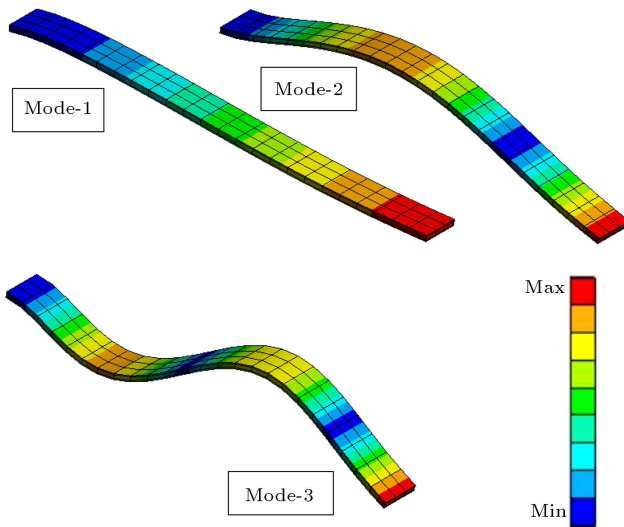


Figure 18. Mode-1, Mode-2, and Mode-3 of the cantilever MR sandwich beam.

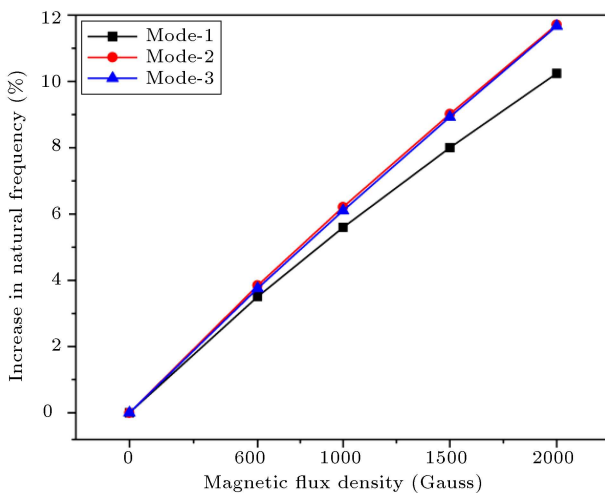


Figure 19. Percentage of change in the natural frequency with the magnetic field.

transient studies were performed for the carbon/epoxy composite sandwich beams with the in-house prepared MR fluid samples. The effects of face layer thickness, core thickness, Carbonyl Iron (CI) particle volume percentage, and magnetic field on the vibrational response of the sandwich beam were presented. The results obtained in this current research work are summarized as follows:

- In the strain amplitude sweep test, the storage modulus decreased, while the loss factor increased as the strain amplitude increased;
- The CI particle volume fraction percentage in the MR fluid had a strong influence on the rheological properties. The storage modulus was higher in value at the higher volume percentage of CI particle MR fluid;
- The amplitude of vibration decreased as the core thickness increased and also, there was a left shift in the frequency curve of the MR fluid sandwich beam. The settling time response of the sandwich beam also improved with core thickness;
- There was a right shift in the frequency response curve observed as the face layer thickness increased. This is due to an increase in the stiffness of the sandwich beam with the thickness of the face layer;
- The higher CI particles, MR fluid sample improved the natural frequency of the sandwich beam and also showed a significant reduction in the vibration amplitude;
- The natural frequency of the composite sandwich beam increased as the magnetic field increased. At higher modes, the difference in natural frequency was greater than that at the lower modes.

Nomenclature

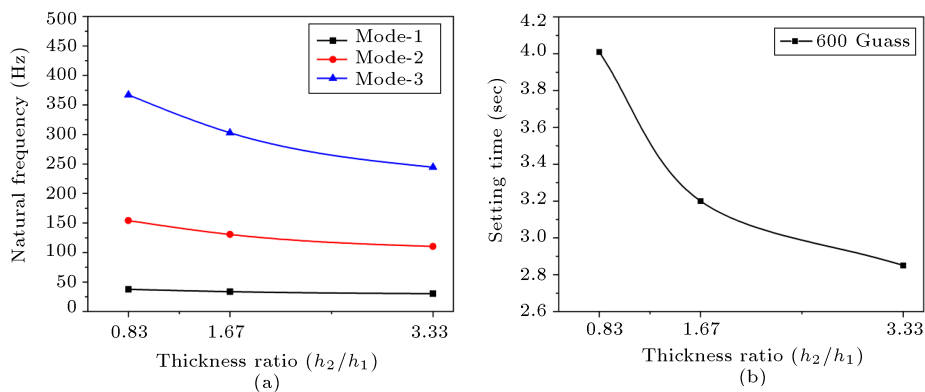
<i>MR</i>	Magnetorheological
<i>CI</i>	Carbonyl Iron
Vol%	Volume percentage
SEM	Scanning Electron Microscopy
PSD	Particle Size Distribution
MRD	Magnetorheological Device
$G'(B)$	Storage modulus
$G''(B)$	Loss modulus
$G^*(B)$	Complex shear modulus
$\eta(B)$	Loss factor
ACP	ANSYS Composite Pre-post

Acknowledgment

The authors acknowledge the support from the Department of Science and Technology (DST) file no.

Table 5. Natural frequencies of the two different fluid MR sandwich beams in various magnetic fields.

Mode	Magnetic field (Gauss)	Natural frequency (Hz)	
		S-II sample	S-I sample
Mode-1	0	22.939	25.783
	600	23.849	26.687
	1000	24.396	27.226
	1500	25.046	27.846
	2000	25.643	28.424
Mode-2	0	79.024	89.042
	600	82.121	92.464
	1000	84.027	94.573
	1500	86.344	97.072
	2000	88.522	99.471
Mode-3	0	160.47	179.3
	600	166.14	186.03
	1000	169.7	190.24
	1500	174.1	195.3
	2000	178.29	200.22

**Figure 20.** Influence of thickness ratio (h_2/h_1) on (a) natural frequency and (b) settling time.

ECR/2016/001448 titled “Experimental Investigation of Passive, Semi-active and Active vibration control of Composite Sandwich Structure” funded by Science and Engineering Research Board, Government of India.

References

- Rabinow, J. “The magnetic fluid clutch”, *Trans. Am. Inst. Electr. Eng.*, **67**, pp. 1308–1315 (1948).
- Ashtiani, M., Hashemabadi, S.H., and Ghaffari, A. “A review on the magnetorheological fluid preparation and stabilization”, *J. Magn. Magn. Mater.*, **374**, pp. 711–715 (2015).
- Kolekar, S., Venkatesh, K., Oh, J.S., et al. “Vibration controllability of sandwich structures with smart materials of electrorheological fluids and magnetorheological materials: A Review”, *J. Vib. Eng. Technol.*, **7**(4), pp. 359–377 (2019).
- Kciuk, M. and Turczyn, R. “Properties and applications of magnetorheological fluids”, *Frat. ed Integrita Strutt.*, **23**(May 2014), pp. 57–61 (2012).
- Iglesias, G.R., López-López, M.T., Durán, J.D.G., et al. “Dynamic characterization of extremely bidisperse magnetorheological fluids”, *J. Colloid Interface Sci.*, **377**(1), pp. 153–159 (2012).
- Hajalilou, A., Amri Mazlan, S., Lavvafi, H., et al., *Field Responsive Fluids as Smart Materials*, Singapore: Springer (2016).
- Kumar Kariganaur, A., Kumar, H., and Arun, M. “Effect of temperature on sedimentation stability and flow characteristics of magnetorheological fluids with damper as the performance analyser”, *J. Magn. Magn. Mater.*, **555**(April), 169342 (2022).
- Kumar Kariganaur, A., Kumar, H., and Arun, M. “Influence of temperature on magnetorheological fluid

- properties and damping performance”, *Smart Mater. Struct.*, **31**(5), 055018 (2022).
9. Shyam, R., Saini, T., Kumar, H., et al. “Optimal design of flow mode semi-active prosthetic knee dampers”, *Sci. Iran.*, **29**, pp. 1–39 (2022).
 10. Allahverdizadeh, A., Mahjoob, M.J., Nasrollahzadeh, N., et al. “Optimal parameters estimation and vibration control of a viscoelastic adaptive sandwich beam incorporating an electrorheological fluid layer”, *JVC/Journal Vib. Control*, **20**(12), pp. 1855–1868 (2014).
 11. Brooks, D., Goodwin, J., Hjelm, C., et al. “Viscoelastic studies on an electro-rheological fluid”, *Colloids and Surfaces*, **18**(2–4), pp. 293–312 (1986).
 12. Weiss, K.D., Carlson, J.D., and Nixon, D.A. “Viscoelastic properties of magnetorheological and electro-rheological fluids”, *J. Intell. Mater. Syst. Struct.*, **5**(6), pp. 772–775 (1994).
 13. Li, W.H., Chen, G., and Yeo, S.H. “Viscoelastic properties of MR fluids”, *Smart Mater. Struct.*, **8**(4), pp. 460–468 (1999).
 14. Esmailnezhad, E., Jin Choi, H., Schaffie, M., et al. “Rheological analysis of magnetite added carbonyl iron based magnetorheological fluid”, *J. Magn. Magn. Mater.*, **444**, pp. 161–167 (2017).
 15. Yalcintas, M. and Dai, H. “Magnetorheological and electrorheological materials in adaptive structures and their performance comparison”, *Smart Mater. Struct.*, **8**(5), pp. 560–573 (1999).
 16. Yalcintas, M. and Dai, H. “Vibration suppression capabilities of magnetorheological materials based adaptive structures”, *Smart Mater. Struct.*, **13**(1), pp. 1–11 (2004).
 17. Eshaghi, M., Sedaghati, R., and Rakheja, S. “Dynamic characteristics and control of magnetorheological/electrorheological sandwich structures: A state-of-the-art review”, *J. Intell. Mater. Syst. Struct.*, **27**(15), pp. 2003–2037 (2016).
 18. Ahamed, R., Choi, S.B., and Ferdaus, M.M. “A state of art on magneto-rheological materials and their potential applications”, *J. Intell. Mater. Syst. Struct.*, **29**(10), pp. 2051–2095 (2018).
 19. Dyniewicz, B., Bajkowski, J.M., and Bajer, C.I. “Semi-active control of a sandwich beam partially filled with magnetorheological elastomer”, *Mech. Syst. Signal Process.*, **60**, pp. 695–705 (2015).
 20. Taghizadeh, S. and Karamodin, A. “Comparison of adaptive magnetorheological elastomer isolator and elastomeric isolator in near-field and far-field earthquakes”, *Sci. Iran.*, **28**(1A), pp. 15–37 (2021).
 21. Lara-Prieto, V., Parkin, R., Jackson, M., et al. “Vibration characteristics of MR cantilever sandwich beams: Experimental study”, *Smart Mater. Struct.*, **19**(1), 015005 (2010).
 22. Acharya, S., Allien, V.J., N P, P., et al. “Dynamic behavior of sandwich beams with different compositions of magnetorheological fluid core”, *Int. J. Smart Nano Mater.*, **12**(1), pp. 88–106 (2021).
 23. Naji, J., Zabihollah, A., and Behzad, M. “Vibration characteristics of laminated composite beams with magnetorheological layer using layerwise theory”, *Mech. Adv. Mater. Struct.*, **25**(3), pp. 202–211 (2018).
 24. Naji, J., Zabihollah, A., and Behzad, M. “Vibration Behavior of Laminated Composite Beams Integrated with Magnetorheological Fluid Layer”, *J. Mech.*, **33**(4), pp. 417–425 (2017).
 25. Zabihollah, A., Naji, J., and Zareie, S. “Impact Analysis of MR-Laminated Composite Structures”, *Emerg. Trends Mechatronics*, pp. 1–14 (2020).
 26. Rajamohan, V., Sedaghati, R., and Rakheja, S. “Vibration analysis of a multi-layer beam containing magnetorheological fluid”, *Smart Mater. Struct.*, **19**(1), 015013 (2010).
 27. Rajamohan, V., Rakheja, S., and Sedaghati, R. “Vibration analysis of a partially treated multi-layer beam with magnetorheological fluid”, *J. Sound Vib.*, **329**(17), pp. 3451–3469 (2010).
 28. Allien, J.V., Kumar, H., and Desai, V. “Semi-active vibration control of SiC-reinforced Al6082 metal matrix composite sandwich beam with magnetorheological fluid core”, *Proc. Inst. Mech. Eng. Part L J. Mater. Des. Appl.*, **234**(3), pp. 408–424 (2020).
 29. Allien, J.V., Kumar, H., and Desai, V. “Semi-active vibration control of MRF core PMC cantilever sandwich beams: Experimental study”, *Proc. Inst. Mech. Eng. Part L J. Mater. Des. Appl.*, **234**(4), pp. 574–585 (2020).
 30. International, A. “Standard test method for measuring vibration-damping properties of materials E756-9804”, **05**(Reapproved), pp. 1–18 (2017).
 31. Salehi, M., Bakhtiari-Nejad, F., and Besharati, A. “Time-domain analysis of sandwich shells with passive constrained viscoelastic layers”, *Sci. Iran.*, **15**(5), pp. 637–643 (2008).
 32. Sahoo, S.S., Hirwani, C.K., Panda, S.K., et al. “Numerical analysis of vibration and transient behaviour of laminated composite curved shallow shell structure: An experimental validation”, *Sci. Iran.*, **25**(4), pp. 2218–2232 (2018).

Biographies

Suryarao Nagiredla is a PhD scholar at the Department of Mechanical Engineering, National Institute of Technology, Karnataka, India. He has experience in modeling, analysis, and coding using ANSYS, MATLAB, and Python. His research interests include composite materials, sandwich structures, magnetorheological fluids, vibration control, and finite element methods.

Sharnappa Joladarashi received his PhD degree in Mechanical Engineering from Indian Institute of

Technology Madras, Chennai, India in 2008. He is currently working as an Associate Professor at Mechanical Engineering Department at National Institute of Technology Karnataka. He has numerous research articles in the peer reviewed journals. His research interests include composite materials, smart composite sandwich structures, vibration control, and finite element methods.

Hemantha Kumar received his PhD degree in Me-

chanical Engineering from Indian Institute of Technology Madras, Chennai, India in 2009. He is currently working as an Associate Professor at the Mechanical Engineering Department at National Institute of Technology Karnataka. He has led various research projects, supervised 10 PhD Theses, and published numerous research articles in the peer-reviewed journals. His current research interests include vehicular dynamics and vibrations, condition monitoring, and smart fluid and its applications.